Liquid Crystals
Publication details, including instructions for authors and subscription information:
http://www.informaworld.com/smpp/title~content=t713926090

Molecular director and layer response of chevron surface stabilized ferroelectric liquid crystals to low electric field

Paula C. Willis[a]; Noel A. Clark[a]; Cyrus R. Safinya[b]
[a] Condensed Matter Laboratory, Department of Physics and Optoelectronic, Computing Systems Center, University of Colorado at Boulder, Boulder, CO, U.S.A. [b] Corporate Research Laboratories, Exxon Research and Engineering Co., Annandale, New Jersey, U.S.A.

To cite this Article Willis, Paula C. , Clark, Noel A. and Safinya, Cyrus R.(1992) 'Molecular director and layer response of chevron surface stabilized ferroelectric liquid crystals to low electric field', Liquid Crystals, 11: 4, 581 — 592
To link to this Article: DOI: 10.1080/02678299208029012
URL: http://dx.doi.org/10.1080/02678299208029012

LIQUID CRYSTALS, 1992, VOL. 11, NO. 4, 581–592

Molecular director and layer response of chevron surface stabilized ferroelectric liquid crystals to low electric field

by PAULA C. WILLIS*†, NOEL A. CLARK† and CYRUS R. SAFINYA‡

† Condensed Matter Laboratory,
Department of Physics and Optoelectronic Computing Systems Center,
University of Colorado at Boulder, Boulder, CO 80309-0390, U.S.A.
‡ Corporate Research Laboratories, Exxon Research and Engineering Co.,
Annandale, New Jersey 08801, U.S.A.

(*Received 9 April 1991; accepted 15 October 1991*)

Recent papers on chevron surface stabilized ferroelectric liquid crystal cells claim that the chevron layer structure can be reversibly uprighted by application of the low to moderate electric fields typically employed to produce director reorientation. In this paper we show, using optical microscopy and X-ray scattering, that there is no significant change in the smectic layer thickness or chevron layer structure of our chevron surface stabilized ferroelectric liquid crystal cells under typical director switching conditions. Furthermore, we present arguments, based on the known elastic properties of smectics, that there is not likely to be a significant elastic layer response to these levels of applied electric field in any surface stabilized ferroelectric liquid crystal cell with anchored layers. Both the switching and observed continuous optical response to applied field can be understood on the basis of electric field induced reorientation of a non-uniform molecular director distribution. We further show that the typically observed broad distribution of layer orientations about the mean chevron structure arises from localized layering defects.

1. Introduction

Surface stabilized ferroelectric liquid crystal cells are under intense development as electro-optic light valves for optical computing and display applications. A principal aspect of this development has been the effort to understand the ferroelectric chiral Smectic C (S_C^*) layer and director structure under varying alignment and applied field conditions [1–3]. An important class of surface stabilized ferroelectric liquid crystal cells have the so-called chevron layer structure [1], shown in figure 1, in which the smectic layers intersect the bounding plate along parallel lines normal to the direction in which polymer coatings on the plates have been rubbed. The chevron arises in the case of interest (ferroelectric liquid crystal material having a Smectic A (S_A) phase at temperatures above the S_C^* phase and a second order S_A–S_C^* transition) from the thermal contraction of the layers, initially planar and normal to the plates in the S_A phase. Because the layers are elastic, resisting thickness strain, and are anchored to the surface, they must buckle into the chevron upon shrinking substantially in thickness [1–3].

It has been recently proposed [4–7] that the electric fields necessary to obtain saturated optical switching (2·5 V/μm for 90 per cent extinction angle saturation in the

* Author for correspondence.

0267–8292/92 $3·00

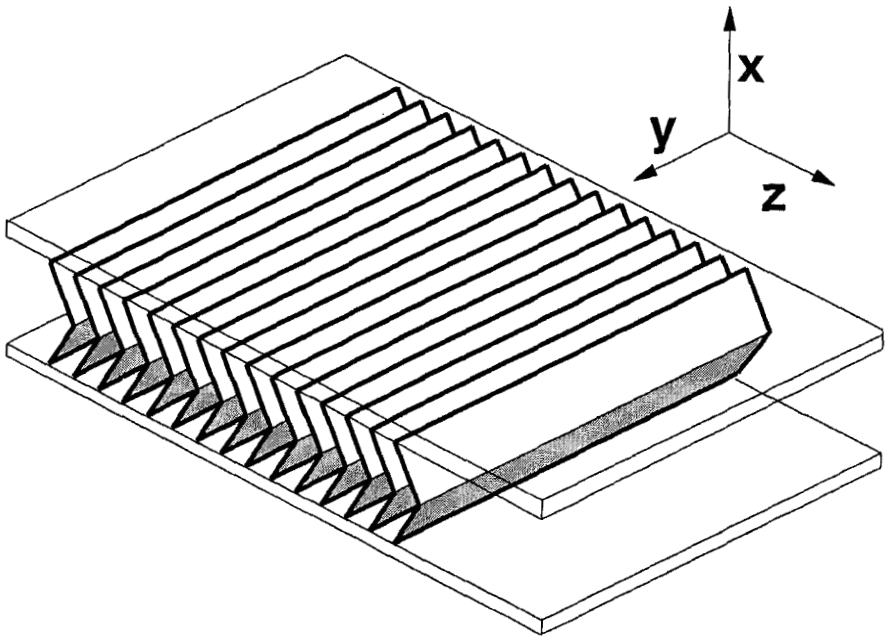

Figure 1. The surface stabilized ferroelectric liquid crystal chevron layer structure.

Chisso 1014 ferroelectric liquid crystal mixture studied here) produce marked changes in smectic layer structure. Specifically it was suggested that the chevroned layers flatten elastically, becoming more normal to the plates in the bulk of the cell while the field is applied, and reversibly returning to the initial chevron when the field is removed. This proposal, coupled with the assumption that the director n of the material remains everywhere parallel to the substrate surfaces when a field is applied to the cell, was put forward to explain the increase of the extinction angle with increasing electric field, i.e. the angle between the smectic layer normal and the polarizer direction when the cell is placed between crossed polarizers and oriented to visually minimize the light transmitted.

In this paper we present X-ray scattering and optical microscopy results which show that in our cells for electric fields at or below values needed for saturated optical switching, the field induced layer structure alteration is minimal and largely plastic. Here, 'saturated optical switching' refers to the state characterized by an asymptotic extinction angle which is approached as the applied voltage is increased (10 V DC effectively saturates the optical response in the cells used). We find the elastic changes in layer structure to be barely detectable at these voltages, in agreement with theoretical estimates, and also discuss the observable plastic changes in both chevron angle and layer thickness. The optical effects noted previously can be explained by the electric field response of the non-uniform (half splayed) $\hat{\mathbf{n}}-\mathbf{P}$ distribution of the chevron cell [8,9], where $\hat{\mathbf{n}}-\mathbf{P}$ is the coupled director-polarization field in the cell (see § 2). The optical and X-ray scattering results are shown to be compatible with a model based on known S_C^* elastic properties, which indicates that elastic forces can balance the field induced torques on the layers with little layer distortion, assuming that the layer anchoring conserves the layer pitch along z and prevents plastic layer rotation about the x axis from releasing the field induced dilative strain. At sufficiently high fields these

conditions break down, leading to plastic flow and locally restructured layers often in the form of line defects known as field lines, boat wakes or roof tops [10]. The structure of these defects has been deduced by optical microscopy and X-ray scattering and will be discussed in a separate publication [11].

2. X-ray and optical experiments; principal results

Figures 2, 4, 6, and 7 summarize the experimental results. Surface stabilized ferroelectric liquid crystal cells were prepared using the Chisso Chemical Co. mixture CS1014 in a 1·8 μm thick gap between glass cover slips with rubbed nylon alignment layers. The phase sequence of CS1014 is

$$X - 21°C\ S_C^* \ 54°C\ S_A \ 69°C\ N^* \ 81°C\ I.$$

The cells were cooled from the S_A phase to form a chevron texture in the S_C^* phase which was studied at $T \sim 27°C$. The cell's alignment was reasonably good, with the optical contrast under white light at 2 V being 100:1 at the time of the optical measurements. Optical measurements were made with a Nikon Optiphot-Pol microscope with polarizer and analyser 90° to one another. To measure extinction brightness (see figure 3) and angle, DC electric fields were applied to the cell and the cell oriented from having the layer normal along the polarizer axis through the angle α to obtain maximum extinction between crossed polarizers (see figure 2). Transmitting states were measured with the cell rotated to extinction angles α and voltages V as indicated in figure 2, but with the applied voltage reversed in polarity [12].

Theoretical extinction angle curves as a function of voltage, $\alpha(V)$, were generated as follows: we used the 4×4 Berreman matrix approach to calculate the transmission spectra of the model cell under varying voltage and orientation conditions, $T(\lambda, V, \alpha)$.

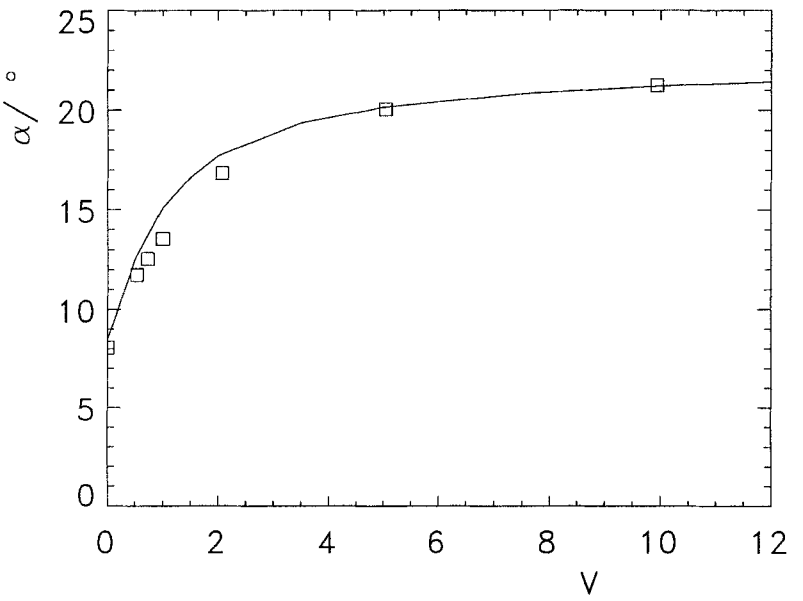

Figure 2. Extinction angle α versus applied voltage. □ our experimental data; —— model prediction.

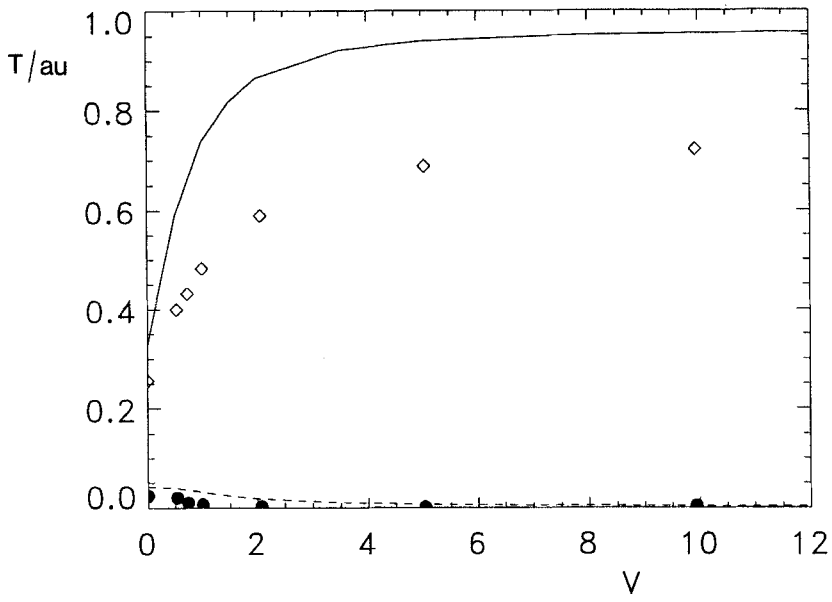

Figure 3. Transmission, T, versus applied voltage, data and theory. ◇ bright (transmitting) state, experimental; —— bright state, theory; ● dark (extinguishing) state, experimental; ---- dark state, theory.

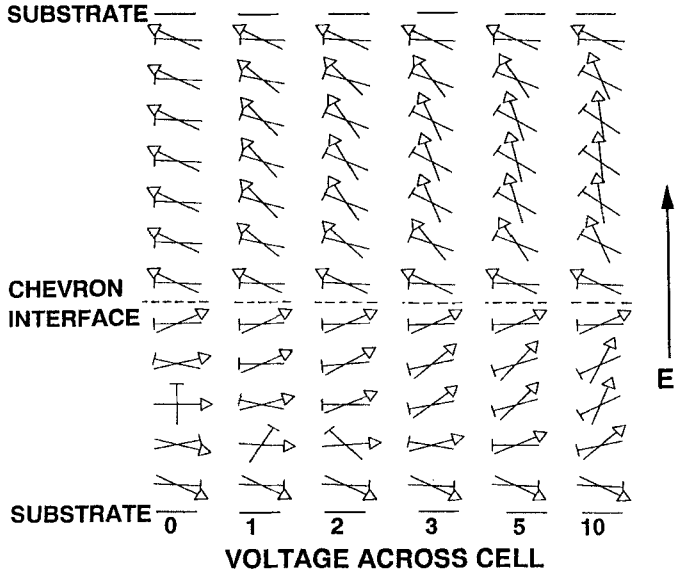

Figure 4. The modelled $\hat{\mathbf{n}}-\mathbf{P}$ (director-polarization) field distribution demonstrated in this article to explain the observed optical and X-ray data. The arrows indicate the molecular polarization field. The line segments on each arrow represent the director field, with a cross-bar denoting the end of the director projecting out of the page. For clarity, the fields are represented as they would appear projected on to the xy plane.

These calculations took into account the ferroelectric liquid crystal's Frank elastic coefficients, Chisso 1014 material and cell parameters, and director boundary conditions expected at the substrate and chevron interfaces [8,9]. No layer flexing, only $\hat{\mathbf{n}}-\mathbf{P}$ changes, existed in our model. The calculated $\hat{\mathbf{n}}-\mathbf{P}$ distribution and its evolution with applied field is shown in figure 4. This approach was based on the interlayer elasticities that exist in typical surface stabilized ferroelectric liquid crystal materials (see § 3.3). From $T(\lambda, V, \alpha)$ we generated $B(V, \alpha)$, the visual brightness (see figure 3) for a given voltage V and cell orientation α

$$B(V,\alpha)=\int T(\lambda, V, \alpha)\times R(\lambda)d\lambda,$$

where $R(\lambda)$ is the light-adapted human eye's spectral response [13]. Finally, the extinction angle at voltage V_1, $\alpha_x(V_1)$,

$$\alpha_x(V_1)=\min\{B(V_1,\alpha)\},$$

was the minimum point of the visual brightness versus orientation curve for $V=V_1$.

The principal evidence for the proposal of [4] is the dependence of the cell extinction orientation on applied electric field. Figure 2 shows this data for our Chisso 1014 cell, which is qualitatively the same as that given in [4]. This dependence of extinction angle on applied field, however, may be understood by considering only the dependence of $\hat{\mathbf{n}}-\mathbf{P}$ on applied field, $\mathbf{E}$.

To illustrate this, we numerically calculated extinction orientation versus $\mathbf{E}$ based only on $\hat{\mathbf{n}}-\mathbf{P}$ changes, assuming no layer response, as described above. The resulting curve shows an excellent match to experimental data, as is shown in figure 2. The apparent extinction angle increases with increasing voltage and with ± 10 volts applied, reaches $\pm 21{\cdot}2°$, 94 per cent of its saturation value, observed to be 22°, as expected for CS1014. We would expect to see approximately flat chevron layers at this voltage, if layer flattening were the cause of extinction angle changes. Interestingly, however, applied voltages in this range produce almost no elastic changes in $I_\beta(\beta)$ and $I_{2\Theta}(2\Theta)$, as can be seen from figures 6 and 7.

Figure 3 shows a good qualitative fit between experimental data and theoretical predictions for the visual transmission curves of the cell in its extinct and transmitting states. The experimental curves are similar to those for the cell of [4] (which appear in [12]), as we expect for cells with the same field response mechanism [14].

The greater dark state transmission in our cells relative to those of [12] is due to the increased thickness of our cells, which allows in this case more visible light leakage. This is due to the smaller cut off wavelength for Mauguin propagation [9] in the thinner cells, which contributes to the light leakage often observed in thicker 3 μm cells under 0 V as a blue dark state. The transmission differences between modelled and experimental bright states may be due to local slight imperfections in layer orientation existing in this cell, as observed both visually and from the unimpressive 100:1 extinction ratio. Visual observations revealed small spots with extinction angles and other visual characteristics rotated about 2° in χ from the background layers. All experimental spectral transmission curves were well-matched qualitatively, however, by our model's predicted spectral transmission curves. The fit remained good even with varying voltages and cell orientations.

Figure 4 shows $\hat{\mathbf{n}}-\mathbf{P}$ distributions appearing across the cell in our fixed-layer model for varying applied voltages. In the half splayed initial state the splayed portion of the cell reduces the apparent extinction angle from that of a uniformly aligned state.

As the voltage is increased, the $\hat{\mathbf{n}}-\mathbf{P}$ distribution becomes more uniform, and the apparent extinction angle approaches that of a cell having a uniform $\hat{\mathbf{n}}-\mathbf{P}$ field.

The X-ray scattering experiments were carried out at Brookhaven National Laboratory's National Synchrotron Light Source on beamline X10B using a diffractometer essentially as described in [15]. The X-ray wavelength was 1·58 Å.

The layering in each local volume element of the sample can be specified by giving its tilt angle β and layer spacing $d(2\Theta)=\pi/(K_i \sin 2\Theta)\cong\pi/(K_i 2\Theta)$, which will determine the scattering angle 2Θ (see figure 5) from that volume element. The scattered X-ray intensity $I(\beta, 2\Theta)$ then is a function of the two variables β and 2Θ, and is proportional to the local distribution of β and 2Θ in the volume sampled by the X-ray beam. The experiments reported here can be described by a simple joint distribution, with $I(\beta, 2\Theta)$ essentially factoring into independent distributions:

$$I(\beta, 2\Theta)=I_\beta(\beta)\times I_{2\Theta}(2\Theta). \tag{1}$$

Typical forms of $I_\beta(\beta)$ and $I_{2\Theta}(2\Theta)$ are shown in figures 6 and 7 respectively.

The layer orientation distribution $I_\beta(\beta)$ (see figure 6(*a*)) exhibits the double peak indicative of the chevron layer structure, in this case an asymmetric chevron with the chevron interface 0·4 t from one surface, where t is the ferroelectric liquid crystal thickness, and 0·4 t is determined from a comparison of the two $I_\beta(\beta)$ peak areas. The distribution $I_{2\Theta}(2\Theta)$ is extremely sharp (full width at half maximum in $2\Theta=0{\cdot}012°$), a result of (1) the spectrometer angular resolution ($\Delta(2\Theta)=0{\cdot}010°$, determined by the graphite analyser crystal), and (2) the uniformity of smectic layer spacing $d\pm(\Delta d/2)$ in the cell $[(\Delta d/d)=(-\Delta 2\Theta/2\Theta)<0{\cdot}004]$. The distributions $I_{2\Theta}(2\Theta)$ of figure 7 were obtained with $\beta\sim 18°$, the taller peak's apex position in $I_\beta(\beta)$. Note that the data show, and equation (1) implies, that layer spacing is independent of layer orientation. Thus the peak shape of $I_{2\Theta}(2\Theta)$ does not observably change as β is varied from 15° to 21°, for

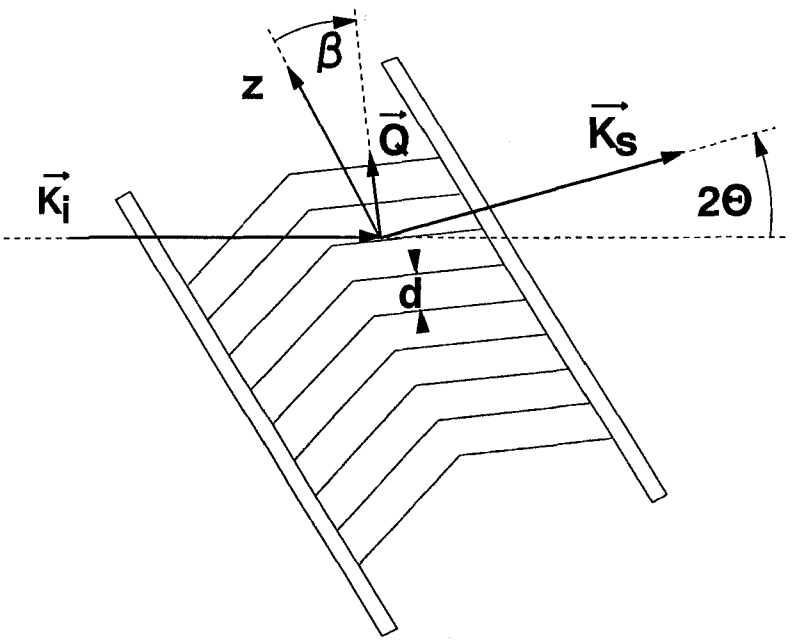

Figure 5. The scattering geometry.

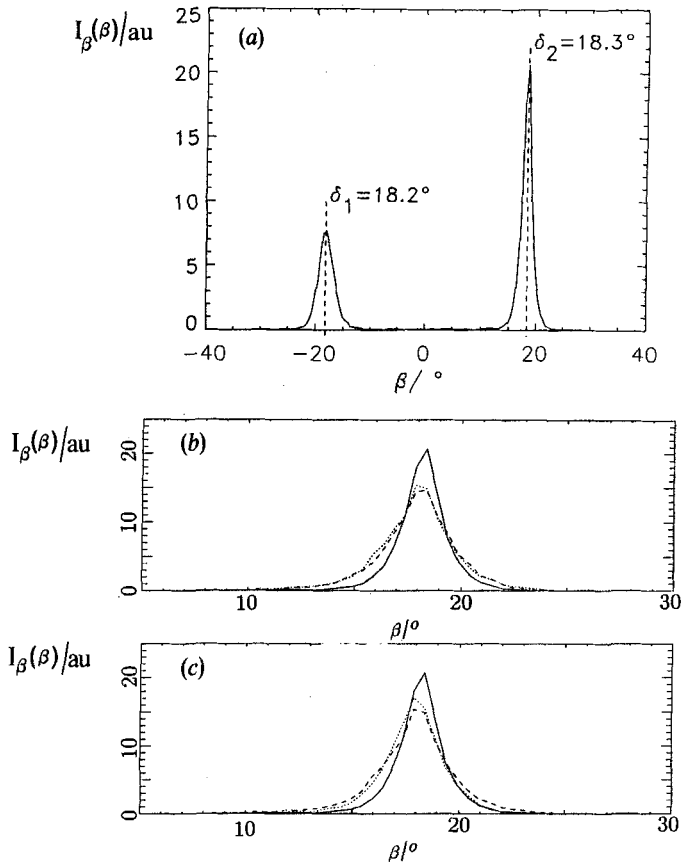

Figure 6. (*a*) The initial chevron cell X-ray scattering intensity distribution, $I_\beta(\beta)$, where δ_1 and δ_2, the peak positions in β, give the **Q** orientations corresponding to the dominant layer normal vectors. Here $|\mathbf{Q}|$ is fixed at $|\mathbf{Q}_0|=(2\pi/d)$, the scattering vector for the S_C layer spacing. The initial stage 2Θ is 3·168°. (*b*) Scattering peaks before applying voltage (——) and during the application of 5 (- - -) and 10 V (....) to the cell. (*c*) Scattering peaks before (——), during (- - -) and after (....) a 10 V application.

The cell is 1·8 μm thick. Note the very small changes in peak position and integrated intensity for both (*b*) and (*c*).

example, in the $I_\beta(\beta)$ peaks enabling the factoring in equation (1). This result is to be expected on the basis of smectic elasticity, as will be discussed later. Figure 6 (*b*) shows the taller $I_\beta(\beta)$ chevron peak of figure 6 (*a*) with 0, 5, and 10 V DC (0, 2·8, 5·6 V μm^{-1}) applied to the cell. Figure 6 (*c*) shows the same peak before, during and after 10 V DC was applied.

The $I_\beta(\beta)$ peak areas in figure 6 are independent of applied voltage. Since for this data $2\Theta_{S_C^*}$ is adjusted to the maximum of the $I_{2\Theta}(2\Theta)$ peak, the field independence of the $I_\beta(\beta)$ area indicates that the $I(2\Theta)$ peak position and therefore d do not shift with voltage. Since the $I(2\Theta)$ peak is so sharp, the $I_\beta(\beta)$ area is a sensitive indicator of shifts in d. For the various data in figure 6, d is constant to within 1 part in 10^3 by this indicator.

$I_{2\Theta}(2\Theta)$ before, and then after 5 and 10 V DC applications are shown in figure 7. The starting peak positions of figure 6 (*a*) give mean layer tilts for the starting chevron of

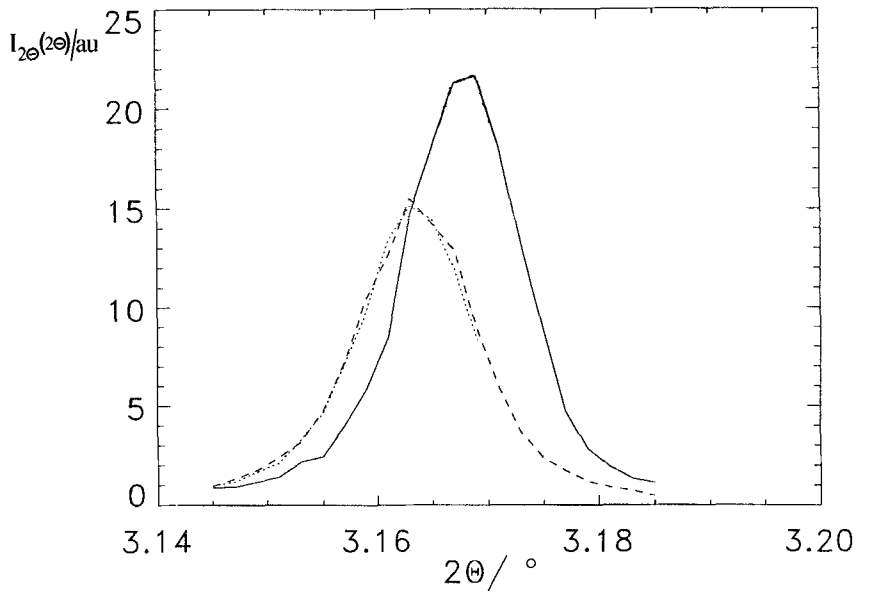

Figure 7. $I_{2\Theta}(2\Theta)$ at $\beta = 18{\cdot}2°$ initially (——) and also after 5 V (- - -) and then 10 V DC (....) was applied to the cell. The peak width is 1·2 times the resolution limit, indicating that the S_C^* layer spacing d is uniform to within 0·16 per cent.

$\delta = -18{\cdot}3°$ and $18{\cdot}2°$, which are reasonably consistent with the chevron rules. That is, given our measured values of $d_{S_C^*} = 28{\cdot}6$ Å, $d_{S_A} = 30{\cdot}3$ Å, and

$$d_{S_C^*} = d_{S_A} \cos \delta, \tag{2}$$

we find $\delta = 19{\cdot}3°$. The small shifts observed in $I_\beta(\beta)$ and $I_{2\Theta}(2\Theta)$ of $-0{\cdot}25°$ and $-0{\cdot}0045°$, respectively, between the baseline run and run following a 10 V application appear due to a $\sim 1°$C temperature rise in the experimental chamber.

Note that equation (2) implies a strict correlation between peak location δ in $I_\beta(\beta)$ and the observation point $2\Theta_{S_C^*}$ chosen in $I_{2\Theta}(2\Theta)$, as $(2\Theta)_{S_C^*}$ can be rewritten $(2\Theta)_{S_C^*} = (2\Theta)_{S_A}/\cos\delta$, $(2\Theta)_{S_C^*(S_A)}$ being the 2Θ peak position in the chiral smectic C (smectic A) phase and δ the peak position in $I_\beta(\beta)$. This strict correlation implies a relation between the peak widths in $I_\beta(\beta)$ and $I_{2\Theta}(2\Theta)$ which is not observed, indicating, as will be discussed in § 3.2, that δ and $2\Theta_{S_C^*}$ are locally uncorrelated.

To evaluate the possibility of ion-mediated electric field shielding within the cell during the X-ray experiments, we observed the variation of extinction angle over times comparable to or longer than the X-ray sampling time. We observed only 2° extinction angle relaxation from 19·6° at 5 V DC for such measurements. The observed relaxation corresponds to 50 per cent shielding for a 5 V applied potential (see figure 2). The scattering measurements therefore reflect the layer configuration for field strengths between 50 per cent and 100 per cent of the applied field. For any applied voltage of less than 10 V, this produces a minimum of 80 per cent of the initial optical response, and we can confidently say that there is little layer response for voltages which produce nearly complete optical saturation.

Thus we can explain our observations, and those of [4], of extinction angle dependency on applied field by using only variations of the $\hat{\mathbf{n}} - \mathbf{P}$ distribution.

3. Discussion

3.1. *Comparison to other experimental work*

Related X-ray scattering work by Kuwahara *et al.* [7] experimentally demonstrates layer flexing under much larger electric fields than are needed for 90 per cent optical switching. For example, the 10 MV m^{-1} fields used in their Chisso 1014 cells (see figure 5), which resulted in barely measurable diffraction pattern changes, were 4 times higher than those used to fully switch our Chisso 1014 cells (2·5 MV m^{-1} reaches 90 per cent saturation of the optical response, measured using the extinction angle). The mechanisms they observe are therefore not the mechanisms leading to optical switching. It follows that his last statement, claiming that his results support Wilbert Hartmann *et al.*'s [4] reversible layer bending model proposal for optical switching, is not correct.

More directly applicable is the work of Geißelmann and Zugenmayer [5]. However, they, like Wilbert Hartmann, use a uniform director field model to explain dielectric and optical observations in surface stabilized ferroelectric liquid crystal cells. Because the uniform director field assumption contradicts the results of prior work ([8], in which spectral transmission data and theory were matched, demonstrating the need for splay in the director field of the cells), this simplified model is insufficient to explain extinction angle changes with applied electric field. In addition, they have used extinction measurements from only two cell orientations; this is barely enough for a two-parameter fit, but not enough to double-check the model. In this paper we present a model that not only predicts the observed extinction angle versus voltage behaviour, but also generates spectral transmission curves that qualitatively match data curves for a variety of voltages and cell orientations. Matches such as this between data and theory would make the model of Gießelmann and Zugenmayer more compelling.

3.2. *Chevron rules are satisfied globally, but violated locally*

The X-ray data have revealed a local violation of the chevron rules [1] (i.e. continuous anchored layers having the smectic A pitch along z and no dislocations) based on the broad $I_\beta(\beta)$ peak widths observed. As indicated in the discussion of equation (2) above, the peak positions in $I_\beta(\beta)$ are found to be those expected from $d_{S_C^*}(T)$ in equation (2). However, note that the peak in $I(\beta)$ is rather broad, having a linewidth of $\Delta\beta$ approximately 2° to 3°. This reflects a distribution of layer orientations about some mean value. As there is essentially no instrumental broadening for the $I(\beta)$ scans, the actual layer distribution is represented in this data.

If this $I(\beta)$ peak width were to be achieved while rigorously obeying the chevron rules, either with plane layer chevrons having a distribution of tilts, or with a single chevron having bent layers, then regions having different values of β would have different peak locations in $I_{2\Theta}$. Thus at $\beta = 17{\cdot}7°$ we would expect from equation (2) a peak in $I_{2\Theta}(2\Theta)$ at $2\Theta = 3{\cdot}14°$, and for $\beta = 19{\cdot}9°$ a peak in $I_{2\Theta}(2\Theta)$ at $2\Theta = 3{\cdot}18°$. However, our measurements show that $I_{2\Theta}(2\Theta)$ is essentially independent of β for any given temperature, the peak location in these measurements being $3{\cdot}168° \pm \sim 0{\cdot}002°$ for all sampling locations in β. Thus the $I_\beta(\beta)$ distribution is achieved with layer elements having the equilibrium layer thickness everywhere, i.e. without the substantial layer strain which the broad $I_\beta(\beta)$ distribution and universal enforcement of the chevron rule would require. Note that this shows that progressive summing of the $I_\beta(\beta)$ distribution to get layer profiles [16] is essentially incorrect.

This result indicates the presence of layering defects which enable a local layer reorientation without the layer strain required by equation (2). These might be edge dislocations, but they would have to be bound somehow, since free dislocation motion would globally relax the chevron rules.

3.3. *Estimate of layer elastic response*

Figures 6(*c*) and 7 show that upon removal of the applied 10 V field, there is little observable elastic relaxation back to the 0 V structure. The very small relaxation of $I_\beta(\beta)$ and $I_{2\Theta}(2\Theta)$ upon removal of the electric field is evidence of a correspondingly small field induced elastic deformation of the layering. This is consistent with the known elastic properties of smectic phases, which may be seen in the following calculation.

We assume here that the field has already reoriented $\hat{\mathbf{n}}-\mathbf{P}$ within the chevron layers to maximize $\mathbf{P}\cdot\mathbf{E}$. This leaves the layer tilt angle, δ, between $\mathbf{P}$ and $\mathbf{E}$, resulting in a spatially uniform electrostatic energy density of $U_e=-PE\cos\delta$. The overall energy density, U, has another term, that of the layer compressional elasticity

$$U_c=\frac{B}{2}\left(\frac{\Delta d}{d}\right)^2,$$

where B is the layer compressional elastic constant, and $(\Delta d/d)$ is the layer compressional strain. Therefore

$$U=U_e+U_c=-PE\cos\delta+\frac{B}{2}\left(\frac{\cos\delta-\cos\delta_0}{\cos\delta_0}\right)^2,$$

where δ and δ_0 are the mean chevron layer tilt angles with and without an applied field. Minimizing $U(\delta)$ gives

$$\Delta\delta=\delta_0-\delta=\frac{PE}{B}\frac{\cos^2\delta_0}{\delta_0}, \tag{3}$$

where for numerical purposes we have used values of Chisso 1014 ($\mathbf{P}=-5{\cdot}4\,\mathrm{nC\,cm^{-2}}=-54\,\mu\mathrm{C\,m^{-2}}$, $\delta_0=18{\cdot}3^\circ=0{\cdot}319$ rad), and we estimate B from typical smectics at temperatures well below the nematic to S_A transition ($B\geqslant 6{\cdot}5\times10^7$ dynes $\mathrm{cm^{-2}}=6{\cdot}5\,\mathrm{MJ\,m^{-2}}$ [17]).

With these values in equation (3), we expect only a small elastic response ($\Delta\delta<-0{\cdot}008^\circ$) for 0 to 10 V on this 1·8 μm thick cell. This gives $(\Delta d/d)=-(\tan\delta)\Delta\delta\cong 4{\cdot}3\times10^{-5}$, a value far smaller than our experimental resolution allows and far less than our 2Θ observed plastic layer thickness change of $(\Delta d/d)=0{\cdot}0016$, discussed in § 3.2.

It is appropriate to mention here that dramatic layer flexing has been predicted by A. MacGregor [6]. His calculation, however, inappropriately leaves out the layer compressional elasticity term, which dominates resistance to layer flexing in our simplified consideration. Comparison of the elastic free energy density in his paper, equation (9), to Dahl and Lagerwall's equations (7–11) [18] shows that the layer compressional elasticity term $\bar{B}\gamma^2$ is left out. Implicit in dropping this term is the assumption that the stresses in the layer structure occurring for field induced director reorientation are too small to produce significant layer compression. The $\bar{B}\gamma^2$ term can then be dropped and the layer spacing fixed at its equilibrium value. This assumption is essentially consistent with our data. However, MacGregor in his calculation apparently dropped the $\bar{B}\gamma^2$ term and still allowed the layer spacing to change, producing in his model an anomalously large layer compression.

3.4. *Plastic zig-zag wall motion*

The small field-induced layer response observed here is also consistent with expected elastic properties of zig-zag walls subjected to electric fields in an unchanging chevron layer structure. Zig-zag walls are the line defects mediating the change in chevron direction [2]. Analysis of the zig-zag defect structures show that they enable the chevron direction to change while everywhere maintaining the S_C^* layer thickness and connection [2, 3].

Layer flexing [3] would require massive changes in zig-zag wall structure to maintain these conditions. However, the zig-zag defects show no visible elastic changes related to application of these low electric fields. This is consistent with our expectations based on elastic interlayer interactions and a resulting infinitesimal layer flex. Inelastic zig-zag wall responses are common; these plastic responses appear due to localized dislocation motion.

4. Summary

To summarize, we have explained our observations of extinction angle dependency on applied field using only variations of the $\hat{\mathbf{n}} - \mathbf{P}$ distribution. Observable elastic layer flexing is not expected energetically, and is not seen, either directly, with X-ray scattering, not indirectly, via zig-zag wall elastic responses. In our judgement therefore, elastic layer flexing does not occur in our chevron surface stabilized ferroelectric liquid crystal cells, and is unlikely to occur for electric-field induced states below optical saturation in such cells with the typical interlayer elastic strengths considered here. Exceptionally weak anchoring or high dislocation densities may, however, lead to larger plastic responses at low field than we have found.

The authors would like to acknowledge the able technical support of Mr Steve Bennett at Exxon's NSLS beam lines. This work is supported by NSF Solid State Chemistry grant number DMR 8901657, ARO Center DAAL 03 90-G-0002 and the Optoelectronic Systems Center by NSF Engineering Research Center grant number ECD 9015128 and by the Colorado Advanced Technology Institute (CATI), an agency of the State of Colorado. Brookhaven National Laboratory is supported by the U.S. Department of Energy.

References

[1] Rieker, T. P., Clark, N. A., Smith, G. S., Parmar, D. S., Sirota, E. B., and Safinya, C. R., 1987, *Phys. Rev. Lett.*, **59**, 2658.
[2] Clark, N. A., and Rieker, T. P., 1988, *Phys. Rev.* A, **37**, 1053.
[3] Clark, N. A., Rieker, T. P., and Maclennan, J. E., 1988, *Ferroelectrics*, **85**, 79.
[4] Hartmann, W. J. A. M., Vertogen, G., Gerritsma, C. J., von Sprang, H. A., and Verhulst, A. G. H., 1989, *Europhysics Lett.*, **10**, 657.
[5] Gießelmann, F., and Zugenmaier, P., 1990, *Liq. Crystals*, **8**, 361.
[6] MacGregor, A. R., 1990, *J. mod. Opt.*, **37**, 919.
[7] Kuwahara, M., Kato, M., Idoo, Y., Terasawa, T., Onnagawa, H., and Miyashita, K., 1990, *Proc. 10th European Disp. Res. Conf.*, Amsterdam, p. 154.
[8] Maclennan, J. E., Clark, N. A., Handschy, M. A., and Meadows, M. R., 1990, *Liq. Crystals*, **7**, 753.
[9] Maclennan, J. E., Handschy, M. A., and Clark, N. A., 1990, *Liq. Crystals*, **7**, 787.
[10] Dübal, H. R., Escher, C., and Ohlendorf, D., 1988, *The 12th International Liquid Crystal Conference* (postdeadline paper), Freiburg, West Germany.
[11] Willis, P. C., Xue, Jiu-Zhi, Clark, N. A., and Safinya, C. R., *Jap. J. appl. Phys.* (submitted).
[12] Hartmann, W. J. A. M., 1988, *Ferroelectrics*, **85**, 67.

[13] BOYD, R. W., 1983, *Radiometry and the Detection of Optical Radiation* (Wiley), p. 100.
[14] Transmissions of [12] were measured using a Philips AVP150 photo-multiplier with an S-11 spectral response [HARTMANN, W. J. A. M., 1991 (personal communication)], which peaks at 440 nm and has a FWHM of ~230 nm. We used the human light-adapted visual spectral response to weight our experimental data, which peaks at 550 nm with a linewidth of ~100 nm. Assuming the $\hat{\mathbf{n}} - \mathbf{P}$ and layer response characteristics are the same for the two cells, we do not expect significant qualitative differences to appear in cell transmission curves due to the different spectral weightings.
[15] RIEKER, T. P., 1988, Ph.D. Thesis, University of Colorado, Boulder.
[16] AKAHANE, T., and NAKAMURA, K., 1990, *Proc. of the 13th International Liquid Crystal Conference*, Vancouver, British Columbia, Canada, Book II, 124.
[17] CLARK, N. A., 1976, *Phys. Rev.* A, **14,** 1551.
[18] DAHL, I., and LAGERWALL, S. T., 1984, *Ferroelectrics*, **58,** 215.